

## Two-dimensional photonic crystals designed by evolutionary algorithms

Stefan Preble<sup>a)</sup> and Michal Lipson

*School of Electrical and Computer Engineering, Cornell University, Ithaca, New York 14853*

Hod Lipson

*Schools of Mechanical & Aerospace Engineering and Computing & Information Science, Cornell University, Ithaca, New York 14853*

(Received 27 August 2004; accepted 14 December 2004; published online 3 February 2005)

We use evolutionary algorithms to design photonic crystal structures with large band gaps. Starting from randomly generated photonic crystals, the algorithm yielded a photonic crystal with a band gap (defined as the gap to midgap ratio) as large as 0.3189. This band gap is an improvement of 12.5% over the best human design using the same index contrast platform. © 2005 American Institute of Physics. [DOI: 10.1063/1.1862783]

Photonic crystals (PCs) are structures that possess a photonic band gap<sup>1–3</sup>—a range of frequencies where light is forbidden from propagating in the crystal. By creating defects<sup>1–4</sup> in the PC, light with a frequency in the band gap can be guided or trapped, enabling the control of the flow of light on the nanoscale.<sup>2</sup> The first PCs were not designed and fabricated in a laboratory but were evolved over millions of years in nature. They create the beautiful colors in butterfly wings<sup>5</sup> and are even found in creatures of the sea such as the Sea Mouse.<sup>6</sup> Photonic crystals have traditionally been hand designed by trial and error with some insight from the extensive research of crystalline atomic lattice structures.<sup>2,7</sup> This has yielded simple lattices and unit cells, such as a square lattice of cylinders.<sup>3</sup> The large band gap of these PCs has been achieved by varying the parameters of the lattice,<sup>8</sup> however, it is not known whether these simple structures truly achieve the maximum band gap for a given index contrast.

In this work we use an evolutionary algorithm (EA) to systematically search for PCs with maximal band gaps. EAs are inspired by natural evolution, and operate by repeatedly selecting, varying, and replicating successful individuals in a population of candidate solutions.<sup>9–11</sup> These algorithms are well suited for finding solutions to problems that involve very large and complex search spaces that do not have smooth gradients leading to an optimum. In particular, EAs are well suited for searching open-ended design spaces that are not conveniently characterized by a finite set of parameters, but are spanned instead by an unbounded set of features or primitives, such as the design space of arbitrary functional geometries and morphologies.<sup>12,13</sup>

EAs have been shown to be an effective method for solving problems in photonics. They have been applied to design waveguide and photonic crystal based spot-size converters,<sup>14,15</sup> fiber Bragg gratings,<sup>16</sup> and transitions between traditional index-guided and PC waveguides.<sup>17</sup> They have also been used to obtain the largest reported polarization independent band gap for a two-dimensional square lattice PC.<sup>18</sup> However, the optimized band gap is between very high frequency bands, above the light line, making the crystal implementation in a practical thin dielectric slab impossible.<sup>2</sup>

In this letter we focus only on a photonic crystal with a band gap between the first two bands in order to ensure that the band gap falls under the light line, enabling the fabrication of the crystal in a thin dielectric slab system.<sup>2</sup> The photonic crystal bands were solved by preconditioned conjugate-gradient minimization of the block Rayleigh quotient on a plane wave basis,<sup>19</sup> which was implemented by a freely available software package. From the calculated bands, any band gap (or lack of) was obtained.

An evolutionary algorithm was used to obtain photonic crystals with large band gaps for the TE polarization (electric field in the plane of the photonic crystal) of light. It could easily be applied to the TM polarization, as well. We also only optimized PCs that were based on a square lattice. Starting from randomly generated PCs, the algorithm yielded a PC with a band gap (defined as the gap to midgap ratio, see Fig. 2) as large as  $\Delta f/f_{\text{middle}}=0.3189$ , as shown in Fig. 1(a). The corresponding band diagram is shown in Fig. 2. Also shown in Fig. 1 are the next two best obtained PCs and the best published<sup>8</sup> human design. The human design is a square lattice of square air holes embedded in a high index back-

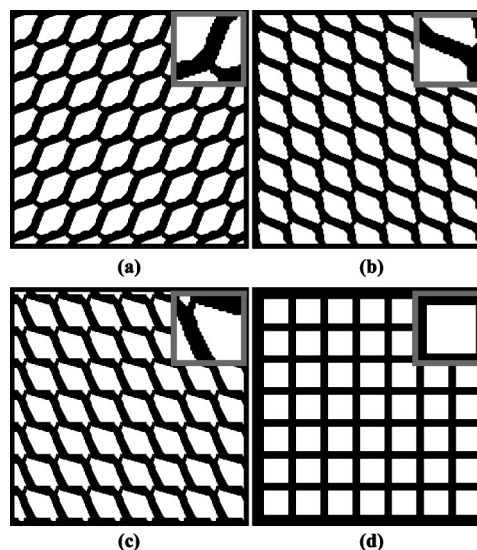


FIG. 1. Photonic crystal and unit cell (insets). (a–c) The best three photonic crystals created by the evolutionary algorithm with the following band gaps: (a) 0.3189, (b) 0.3153, (c) 0.3115. (d) Best human designed photonic crystal with a band gap of 0.2835.

<sup>a)</sup> Author to whom correspondence should be addressed; electronic mail: sfp24@cornell.edu

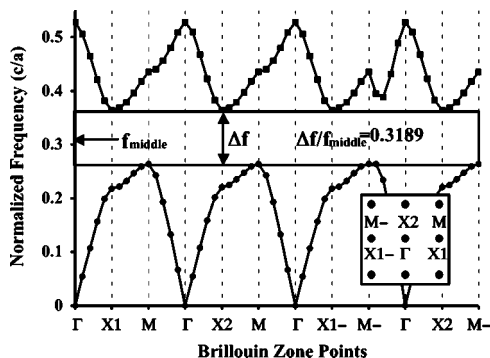


FIG. 2. Band diagram of the best photonic crystal discovered by the evolutionary algorithm. Horizontal axis is the brillouin zone points. The vertical axis is the frequency normalized to the lattice constant. The inset shows the reciprocal lattice and the corresponding Brillouin zone points.

ground. With this index contrast, it has a band gap of only  $\Delta f/f_{\text{middle}}=0.2835$ . Using an evolutionary algorithm, we have therefore improved over the best human design by 12.5%.

It has previously been shown that the band gap of simple photonic crystals can sometimes be improved by reducing the symmetry of the unit cell and the lattice.<sup>8,20,21</sup> By making no assumptions about the symmetry of the unit cell, our evolutionary algorithm has found that the photonic crystals with the largest band gaps have unit cells that lack strong symmetry. Also, the largest known<sup>8</sup> band gap for the TE polarization is obtained using a triangular lattice of hexagonal air holes embedded in a high index background, which resembles a honeycomb structure. With the constraint of a square lattice, the EA attempted to recreate this structure, as seen in Fig. 1. However, the resulting honeycombs are not symmetric; they are skewed and nonuniformly scaled. By doing so the EA was able to find structures that improve over the best human design.

In this letter the unit cell is the element of the photonic crystal that was subject to evolution. The unit cells are discretized onto a  $32 \times 32$  grid of square pixels consisting of high (3.4-silicon) or low (1-air) dielectric material. The EA starts with a population of randomly generated unit cells. Each photonic crystal is obtained by repeating the discretized unit cell on a lattice using a square basis. Any other basis, such as triangular, could in principle be used as well. The fittest photonic crystals, those approaching higher band gaps, are selected and mated with each other. During mating the elements of the parent photonic crystals are crossed over (swapped), and are then subject to mutation (randomly changing high/low dielectric constants). This process is repeated for many generations after which we find photonic crystals with large band gaps.

In general, the initial population of randomly generated PCs does not possess a band gap. In a previous work by He<sup>18</sup> the PCs with no band gap were artificially assigned a small fitness value. A search using such a criterion has no gradient to follow during the initial phase, and therefore drifts blindly in the search space. The lack of gradient may explain why their previous attempt needed to seed the initial population with a hand-designed solution with an existing band gap. Such an approach only has the effect of optimizing the hand-designed solution. In this work we have developed a fitness criterion that is suitable for crystals that do not already possess a band gap, thereby enabling the discovery of new types

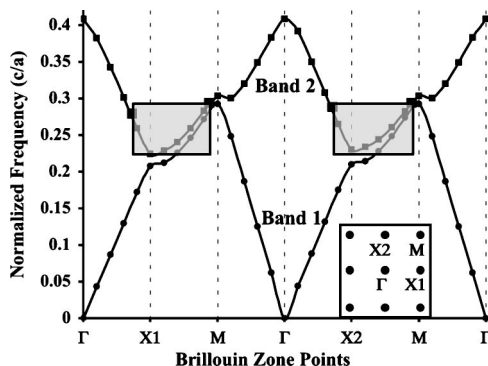


FIG. 3. Band diagram of a randomly generated PC with no band gap. The inset shows the reciprocal lattice and the corresponding Brillouin zone points. The shaded light-gray boxes indicate the areas where the two bands overlap each other. The bounds of the boxes are obtained from the points in the band diagram where the top band is below the top of band 1. The height of the boxes is always the same; it is defined from the bottom of band 2 (At the X1 point) to the top of band 1 (At the M point). The width is from the left-most to the right-most points (including the interpolated halfway points) that fall below the top of band 1. The total overlap area [Eq. (1)] can be obtained from the sum of the areas of the individual shaded boxes.

of PC structures from scratch. Our measure of fitness is the amount of overlap of the top and bottom bands, here referred to as the overlap area, as defined by

$$\text{Overlap Area} = \frac{E_{\text{top},1} - E_{\text{bottom},2}}{(E_{\text{top},1} + E_{\text{bottom},2})/2} \cdot \frac{N_{\text{overlap}}}{N_{\text{total}}}, \quad (1)$$

where  $E_{\text{top},1}$  is the top of the bottom band,  $E_{\text{bottom},2}$  is the bottom of the top band,  $N_{\text{overlap}}$  is the number of calculated Brillouin zone points where the top band is below the top of the bottom band, and  $N_{\text{total}}$  is the total number of points that were sampled in the Brillouin zone. Since no assumptions were made about the symmetry of the unit cell it is necessary to calculate the bands over the entire first Brillouin zone. An example of a PC that does not contain a band gap and how the overlap area is obtained is shown in Fig. 3. Only the Brillouin zone points along the  $\Gamma \rightarrow X1 \rightarrow M \rightarrow X2 \rightarrow \Gamma$  quadrant are shown for compactness. To improve the speed of the band calculations, only four points between each Brillouin zone symmetry point (i.e.,  $\Gamma, X1, M, X2$ ) was calculated, so an additional point is linearly interpolated “halfway” between each one of the points. This interpolation is shown in Fig. 3 where the left and right edges of the two overlap areas do not fall on points that were actually calculated, they fall on the “halfway” points, as indicated by the bold square points (these are the only halfway points shown on this diagram). For PCs that do possess a band gap the fitness criterion used was the gap-to-midgap ratio, as defined by

$$\text{Gap to - Midgap Ratio} = \frac{E_{\text{top}} - E_{\text{bottom}}}{E_{\text{middle}}}, \quad (2)$$

where  $E_{\text{top}}, E_{\text{bottom}}, E_{\text{middle}}$  are the top, bottom and the middle of band gap, respectively.

The evolutionary algorithm does not directly evolve the discretized unit cell representation. Instead, the fast and efficient discovery of photonic crystals with large band gaps is enabled by using an indirect representation. Direct representation in this case are bitmaps, which directly encode the pixelated unit cell. With the bitmap representation there are 1024 ( $32 \times 32$ ) separately encoded pixel elements. With so

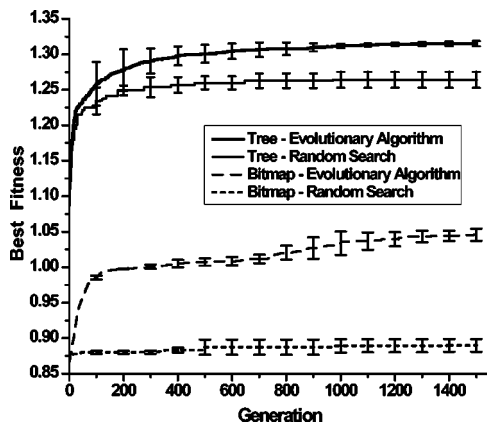


FIG. 4. Best fitness of the population as a function of generation. The tree and bitmap representation performance is compared. A random search is also included as a base line. Error bars are derived from three independent runs started from randomized initial populations.

many elements, the bitmap representation is highly susceptible to noise. The noise has the effect of detracting from the achievable band gap of the PC by reducing its overall index contrast. Alternatively, we used a tree representation that generates the unit cell using a hierarchical set of construction rules. An example rule is to split a section of the unit cell in two, where the section is determined by “split rules” higher up in the tree. The “leaves” of the tree assign a dielectric material to the various sections. Thus, the tree representation defines the unit cell using “clumps” of high or low dielectric material, as opposed to isolated pixels, making it much less susceptible to noise. Unlike bitmaps, tree representations are resolution independent—they can specify any geometry at variable level of detail. To facilitate calculation of the photonic bands, the trees are rasterized onto a  $32 \times 32$  grid, as discussed earlier.

Results of the evolutionary process are seen in Fig. 4 where the best fitness as a function of generation is shown for both the tree and bitmap representations. A fitness below 1 is the overlap area calculated using Eq. (1). A fitness above 1 corresponds to the gap-to-midgap ratio (i.e., a fitness of 1.25 is a 0.25 band gap). Clearly, the tree representation outperforms the bitmap representation by a wide margin. The structures obtained using the bitmap representation are similar to those seen in Fig. 1 but are degraded by a large number of “rogue” pixels that reduce the index contrast. By manually removing these pixels the band gap can be considerably improved. A much larger band gap of  $\sim 0.21$  was obtained by using a much coarser  $16 \times 16$  grid.

Also shown in this graph is a random search (i.e, PCs are randomly generated at each generation, as in the first step of the EA) using both types of representations. The random search with the bitmap representation only yielded “noise,” which has no band gap. However, very good results were achieved when using the random search with the tree representation. This suggests that tree representations are inher-

ently more appropriate for searching this design space. Note that in practice, a combination of direct and indirect representation types may yield the best results. For example, a bitmap representation would work very well for fine tuning small regions of the unit cells obtained from the tree representation.

In conclusion, we have demonstrated the ability to use evolutionary algorithms to discover photonic crystal structures with large band gaps. In contrast to previous works<sup>18</sup> in which the initial population to be evolved was seeded with hand-designed solutions, we evolve a completely random population of PCs that possess very small or even no band gaps. Using this algorithm we obtain PCs with 12.5% larger band gaps than the best human design. As demonstrated by this and previous works, evolutionary algorithms are an effective tool for the design of photonic structures with complex morphologies that have unique optical properties.

The authors acknowledge support by the Cornell Center for Nanoscale Systems, supported by the National Science Foundation (NSF) and by the STC Program of the NSF. This work was performed in part at the Cornell Theory Center which is supported by its users, Cornell University and Industrial Affiliates.

- <sup>1</sup>E. Yablonovitch, Phys. Rev. Lett. **58**, 2059 (1987).
- <sup>2</sup>S. G. Johnson and J. D. Joannopoulos, *Photonic Crystals: The Road from Theory to Practice* (Kluwer, Boston, 2002).
- <sup>3</sup>J. D. Joannopoulos, R. D. Mead, and J. N. Winn, *Photonic Crystals* (Princeton University Press, Princeton, 1995).
- <sup>4</sup>E. Yablonovitch, T. J. Gmitter, R. D. Meade, A. M. Rappe, K. D. Brommer, and J. D. Joannopoulos, Phys. Rev. Lett. **67**, 3380 (1991).
- <sup>5</sup>L. P. Biró, Zs. Bálint, K. Kertész, Z. Vértesy, G. I. Márk, Z. E. Horváth, J. Balázs, D. Méhn, I. Kiricsi, V. Lousse, and J.-P. Vigneron, Phys. Rev. E **67**, 021907 (2003).
- <sup>6</sup>A. R. Parker, R. C. McPhedran, D. R. McKenzie, L. C. Botten, and N. A. Nicorovici, Nature (London) **409**, 36 (2001).
- <sup>7</sup>E. Yablonovitch, J. Opt. Soc. Am. B **10**, 283 (1993).
- <sup>8</sup>N. Susa, J. Appl. Phys. **91**, 3501 (2002).
- <sup>9</sup>J. H. Holland, *Adaptation in Natural and Artificial Systems* (University of Michigan, Ann Arbor, 1975).
- <sup>10</sup>M. Mitchell, *An introduction to Genetic Algorithms* (MIT Press, Cambridge, 1996).
- <sup>11</sup>J. R. Koza, M. A. Keane, M. J. Streeter, W. Mydlowec, J. Yu, and G. Lanza, *Genetic Programming IV. Routine Human-Competitive Machine Intelligence* (Kluwer, Boston, MA, 2003).
- <sup>12</sup>H. Lipson and J. B. Pollack, Nature (London) **406**, 974 (2000).
- <sup>13</sup>H. Lipson, Proceedings of the Genetic and Evolutionary Computation Conference, Seattle, WA, 26–30 June 2004.
- <sup>14</sup>M. M. Spuhler, B. J. Offrein, G.-L. Bona, R. Germann, I. Massarek, and D. Erni, J. Lightwave Technol. **16**, 1680 (1998).
- <sup>15</sup>L. Sanchis, A. Håkansson, D. López-Zanón, J. Bravo-Abad, and José Sánchez-Dehesa, Appl. Phys. Lett. **84**, 4460 (2004).
- <sup>16</sup>S. Manos, L. Poladian, and B. Ashton, Proceedings of the Conference on Laser and Electro Optics/International Quantum Electronics Conference, 16–21 May 2004, San Francisco.
- <sup>17</sup>J. Jiang, J. Cai, G. P. Nordin, and L. Li, Opt. Lett. **28**, 2381 (2003).
- <sup>18</sup>L. Shen, A. Ye, and S. He, Phys. Rev. B **68**, 035109 (2003).
- <sup>19</sup>S. G. Johnson and J. D. Joannopoulos, Opt. Express **8**, 173 (2001).
- <sup>20</sup>C. M. Anderson and K. P. Giapis, Phys. Rev. Lett. **77**, 2949 (1996).
- <sup>21</sup>M. Qui and S. He, Phys. Rev. B **60**, 10610 (1999).